JOTCS A
Journal of the Turkish Chemical Society
Section: A
Chemistry
TURKISH CHEMICAL SOCIETY

Synthesis, Spectroscopic Analysis, and Anti-Bacterial Studies of Pd(II) Complexes of Phosphine and Hydrazone Derivatives

Laith H. K. Al-Jibori and Ahmed S. M. Al-Janabi*

Department of Chemistry, College of Science, Tikrit University, Tikrit, Iraq

Abstract: This study reports the synthesis of seven hydrazone derivative complexes by the treatment equivalent molar of the phosphine ligand $Ph_2P(CH_2)_nPPh_2$ {where n= 1 dppm; n=2 dppe; n=3 dppp; n=4 dppb; $(CH_2)_n$ = $(Cp)_2Fe$} with $[Pd(dbeoz)_2]$ afforded complexes of the type $[Pd(dbeoz)_2(diphos)]$ and $[Pd(dbeoz)_2(dppm)]_2$, whereas the reaction of two moles of Ph3P with $[Pd(dbeoz)_2]$ gave a complex $[Pd(dbeoz)_2(PPh_3)_2]$ in good yield. CHN analysis, conductivity measurements, Fourier Transform Infrared (FT-IR), ^1H, and ^{31}P-NMR, were used to investigate the structural geometries of the complexes. Further, the biological activity of the synthesized complexes was evaluated against three pathogenic bacteria (*Pseudomonas aeruginosa*, *Bacillus subtilis*, and *Escherichia coli*) using the well diffusion method, the synthesized complexes displayed moderate to good inhibitory activity, and the $[Pd(dbeoz)_2(dppf)]$ complex exhibited the highest inhibitory activity with DIZ is 24, 27, and 28 mm against the three pathogenic bacteria, respectively.

Keywords: Hydrazone, phosphine, palladium, metal complexes, anti-bacterial activity

Submitted: August 15, 2023. **Accepted:** November 27, 2023.

Cite this: Al-Jibori LHK, Al-Janabi ASM. Synthesis, Spectroscopic Analysis, and Anti-Bacterial Studies of Pd(II) Complexes of Phosphine and Hydrazone Derivatives. JOTCSA. 2024; 11(1): 245-52.

DOI: https://doi.org/10.18596/jotcsa.1343254.

Corresponding author. Email: dr.ahmed.chem@tu.edu.iq; Mobile: 009647703765962.

1. INTRODUCTION

Hydrazones are compounds that contain the functional group R-NHN=CR', where R and R' can be a variety of substituents. Hydrazones are usually synthesized by heating hydrazides with different aldehydes using solvents such as acetone and ethanol, which can be easily confirmed from its spectral data. Further, they can be used as an intermediate in Wolff Kishner reductions to reduce the carbonyl functionality of aldehyde and ketones into alkanes. Hydrazones can act as versatile ligands in coordination chemistry, forming complexes with transition metals. These complexes can exhibit a range of interesting properties and potential applications (1-2).

Hydrazone derivative ligands can coordinate to a metal center in different modes, such as monodentate, bidentate (chelating), or bridging to a transition metal center through two of its donor atoms. The nitrogen atoms in the hydrazine group can form coordination bonds with the metal center. These different coordination modes can lead to the formation of various complex structures and geometries (2-6). The stability of the produced complexes can vary depending on factors such as the nature of the metal, the coordination mode, and the steric and electronic effects of the ligand. Stability can influence the potential applications of these complexes (1). Hydrazones are readily available, hydrolytically stable, and are enolized only under strongly basic conditions, and they would be attractive partners for radical addition (1,7,8). However, the presence of the second nitrogen decreases the electrophilic character of their C=N bond, resulting in decreased efficiency of adding nucleophilic radicals (1,9,10).

Depending on the specific properties of the Hydrazone derivative complexes, they could find applications in catalysis, sensing, medicinal chem-

istry (such as anti-bacterial, anti-fungi, anti-malaria, etc.), and materials science. For instance, catalytic applications could include oxidation, reduction, and cross-coupling reactions (11-21).

In light of the broad range of applications reported for hydrazone compounds and, as well as its complexes with transition metal ions, Here, we report the synthesis and characterization of a series of Pd(II) hydrazone derivative complexes and evaluation of the biological activity against *Pseudomonas aeruginosa*, *Bacillus subtilis*, and *Escherichia coli* bacteria using the diffusion method.

2. EXPERIMENTAL SECTION

2.1 Materials and Apparatus

The chemical compounds and solvent provided were employed without undergoing purification. UV-visible spectra were evaluated within the 900 to 200 nm range utilizing a Cary 100 spectrophotometer in DMSO solutions. FT-IR spectra were recorded 400 to 4000 cm^{-1}, employing KBr discs on a SHIMADZU FT-IR apparatus. Molar conductance was gauged in a DMSO solution at a 10^{-3} M temperature of 25 °C using an Oakton EC Tester 11 dual-range conductivity tester. The NMR spectra were measured using a Bruker 400 MHz spectrometer, with DMSO-d6 as the solvent.

2.2 General Procedure of the Preparation of Complexes

A solution of $Ph_2P(CH_2)_nPPh_2$ (0.063 mmole) or Ph_3P (0.126 mmole) in EtOH (10 mL) was added to a suspension of $[Pd(dbeoz)_2]$ (0.05 g; 0.063 mmol) in EtOH (10 mL), a colored solution was formed. The mixture was stirred for four hours, during which a color precipitate formed. The stirring was continued until the designated time elapsed. The solution was filtered and washed with distilled water, followed by ether and ethanol. The precipitate was dried under reduced pressure, and it was crystallized from DMSO (Schemes 1 and 2). The color, yield percentage, m.p. (°C), and other physical properties are listed in Table 1.

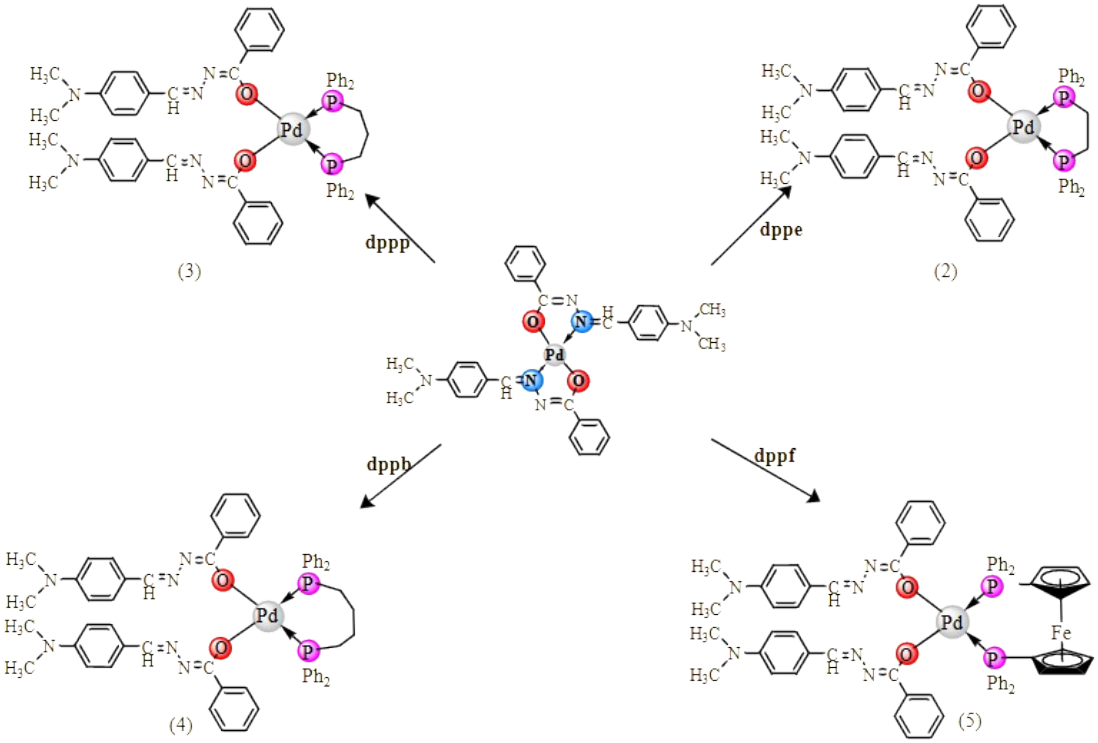

Scheme 1: Preparation of Pd(II) complexes (**2-5**).

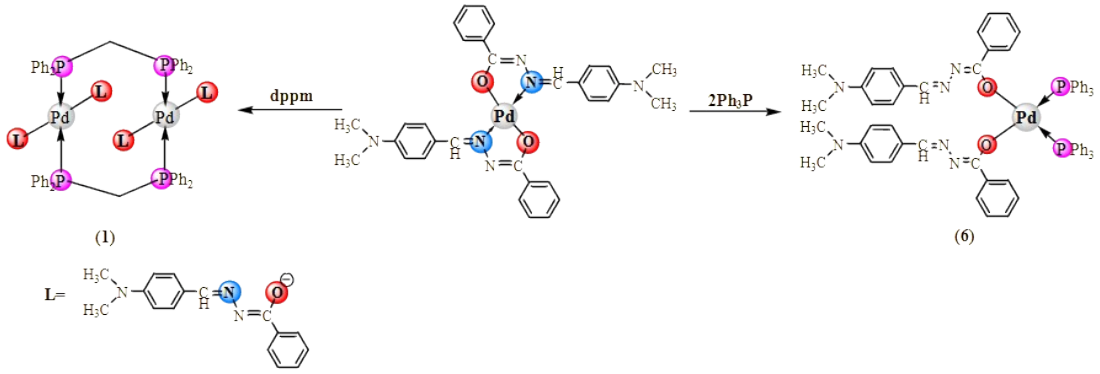

Scheme 2: Preparation of Pd(II) complexes (**1** and **6**).

2.3 Anti-Bacterial Activity

The anti-bacterial activity of the synthesized complexes was assessed against three bacterial strains, namely *Pseudomonas aeruginosa*, *Bacillus subtilis*, and *Escherichia coli*, using the disc diffusion method on the nutrient agar described by Bauer (22). Six synthesized complexes were evaluated at a concentration of 10^{-3} M in DMSO solution, and the results were compared with Tetracycline and dimethyl sulphoxide (DMSO), which were used as positive and negative controls, respectively.

3. RESULTS AND DISCUSSION

3.1 Synthesis

The complexes [Pd(dbeoz)$_2$(diphos)] and [Pd (dbeoz)$_2$(dppm)]$_2$ were prepared by reacting equivalent molar of the diphosphine ligands with [Pd(dbeoz)$_2$] in ethanol as a solvent (Scheme 1) to afford a green complex with the dppm ligand, an orange complex with the dppe ligand, and a red complex with the dppp ligand. Additionally, a brown complex was obtained with the dppf ligand. On the other hand, the complex [Pd(dbeoz)$_2$(PPh$_3$)$_2$] was prepared by treatment of two equivalent moles of the triphenylphosphine ligand (PPh$_3$), with [Pd(dbeoz)$_2$] to afford an olive complex (Scheme 2). The results indicate that the HDmby ligand was coordinated as a monodentate ligand via the oxygen atom of the carbonyl group. The molar conductivity results for the complexes are listed in Table 1, indicating that all complexes were non-conductive, suggesting their non-electrolytic complexes. Furthermore, the elemental analysis results were consistent with the proposed formulas of the prepared complexes.

Table 1: Some of the physical properties and CHN analysis of the synthesized complexes.

No	Complexes	Color	Λ*	m.p (°C)	Yield %	Elemental analysis (CHN) Calc.(found)		
						C	H	N
1	[Pd(Dmby)$_2$(dppm)]$_2$	Green	10.0	300-303	51	66.89 (67.07)	5.32 (5.43)	8.21 (8.50)
2	[Pd(Dmby)$_2$(dppe)]	Orange	11.0	257-259	91	67.15 (67.08)	5.44 (5.32)	8.10 (8.37)
3	[Pd(Dmby)$_2$(dppp)]	Red	6.8	287-288	80	67.39 (67.56)	5.56 (5.62)	7.99 (8.13)
4	[Pd(Dmby)$_2$(dppb)]	Orange	7.0	297-300	54	67.63 (67.78)	5.68 (5.92)	7.89 (7.94)
5	[Pd(Dmby)$_2$(dppf)]	Brown	8.0	282-283	30	66.42 (66.51)	5.07 (5.28)	7.04 (7.23)
6	[Pd (Dmby)$_2$(PPh$_3$)$_2$]	Olive	2.4	291-293	56	70.19 (70.23)	5.37 (5.43)	7.22 (7.49)

* molar conductivity was measured in DMSO solution at 10^{-3} in (ohm^{-1}. cm^2. mol^{-1})

3.2 Spectral data

3.2.1 IR data

The infrared spectra of [Pd(dbeoz)$_2$(dppm)]$_2$, [Pd(dbeoz)$_2$(diphos)], and [Pd(dbeoz)$_2$(PPh$_3$)$_2$] (Figures SI 1-4) have revealed three characteristic bands that were absent in the spectrum of complex [Pd(dbeoz)$_2$]. These bands confirm complex formation and the incorporation of phosphine ligands within their structures. Specifically, these bands due to ν(P-Ph), ν(P-C), and ρ(P-C) which displayed within (1433-1456) cm^{-1}, (1064-1099) cm^{-1}, and (493-509) cm^{-1}, range, respectively (23-25).

A slight shift in the carbonyl group stretching frequency was noted within the range of (1645-1670) cm^{-1}, suggesting the coordination of the ligand ($dbeoz^-$) via the oxygen atom of the carbonyl group. In contrast, the stretching frequency of the azomethine group has been displaced to a slightly higher wavenumber than in the complex $[Pd(dbeoz)_2]$ (1567 cm^{-1}), appearing within the range of (1600-1610) cm^{-1}, approximating or slightly surpassing that of the free ligand. This indicates its lack of involvement in coordination with the Pd(II) ion, thereby supporting the proposed monodentate fashion of the ligand $dbeoz^-$ via the oxygen of the carbonyl group (26-31). New bands have been observed in the prepared complexes due to the ν(Pd-P) and ν(Pd-O), which displayed within the ranges of (455-486) cm^{-1} and (418-443) cm^{-1}, respectively (24-28). Further, the IR spectra displayed the ν(C-H)aromatic and ν(C-H)aliphatic within the range of (3051-3059) cm^{-1} and (2804-2987) cm^{-1}, respectively.

3.2.2 ^{31}P-{^1H} and ^1H NMR data

The ^{31}P-{^1H}NMR spectra of the prepared complexes (Figure 1) displayed a singlet peak for each complex at δP = 23.70 ppm, 09.61 ppm, 11.95 ppm, 30.03ppm, 25.60 ppm, and 25.53 ppm for the $[Pd(dbeoz)_2(dppm)]_2$, $[Pd(dbeoz)_2(dppe)]$, $[Pd(dbeoz)_2(dppp)]$, $[Pd(dbeoz)_2(dppb)]$, $[Pd(dbeoz)_2(dppf)]$ and $[Pd(dbeoz)_2(PPh_3)_2]$, respectively. The presence of a singlet peak indicates the existence of a single isomer, and the phosphorus atoms are equivalent (23-25).

Table 2. IR selected bands (cm^{-1}) of the prepared complexes.

Band assignment	Complexes						
	$[Pd(dbeoz)_2]$	**1**	**2**	**3**	**4**	**5**	**6**
$\nu(C\text{-}H)_{Ar}$	3059w	3053w	3055w	3051w	3058w	3053w	3053w
$\nu(C\text{-}H)_{aliph.}$	2920w 2856w	2963w 2804w	2891w 2852w	2987w 2893w	2893w 2822w	2964w 2804w	2906w 2858w
ν(C=O)	1604m	1606m	1623m	1615m	1608m	1624m	1616m
ν(C=N)	1577s	1592s	1606s	1596s	1594s	1602s	1593s
ν(C=C)	1523s	1540s	1523s	1523s	1523s	1523s	1523s
ν(P-Ph)	-	1434m	1444m	1433m	1434m	1437m	1456m
ν(P-C)	-	1069s	1064s	1097m	1099m	1097m	1097m
ρ(P-C)	-	505s	513m	509m	505m	493m	507m
ν(Pd-O)	462w	472w	486w	455w	476w	464w	481w
ν(Pd-P)	-	442w	443w	420w	433w	418w	441w

s = strong, m = medium, w= weak.

Clearly, the ^1H NMR spectra of the $[Pd(dbeoz)_2(dppm)]_2$, $[Pd(dbeoz)_2(diphos)]$, and $[Pd(dbeoz)_2(PPh_3)_2]$ complexes (Fig. SI 5-10), indicated that the two dbeoz ligands and phosphine ligands include in the structure complexes. The ^1H NMR spectra displayed the azomethine proton signals at 8.10-8.38 ppm. Meanwhile, protons of the phenyl groups in the dbeoz ligands and diphosphine ligands are displayed as unresolved multiplet peaks in the aromatic region. The results are listed in Table 3.

Table 3: ^{31}P-{^1H}NMR and ^1H NMR data (δ, ppm) of the $[Pd(dbeoz)_2(dppm)]_2$, $[Pd(dbeoz)_2(diphos)]$, and $[Pd(dbeoz)_2(PPh_3)_2]$.

No	Complexes	δP	δH
1	$[Pd(Dmby)_2(dppm)]_2$	23.70	8.35(s, 4H, CH=N); 6.74-8.15(m, 76H); 4.05(t, $J_{H\text{-}P}$ = 13.6Hz, 4H, CH_2-dppm).
2	$[Pd(Dmby)_2(dppe)]$	9.61	8.10(s, 2H, CH=N); 6.35-7.85(m, 38H); 2.75(s, 12H, CH_3); 3.06(s, 24H, $2CH_3$); 2.28(s, 4H, $2CH_2$-dppe).
3	$[Pd(Dmby)_2(dppp)]$	11.95	8.33(s, 2H, CH=N); 7.07-8.07(m, 34H); 6.79(d, J_{HH} = 8.1Hz, 4H); 2.86-3.10(m, 18H, $2CH_2$-dppp+ $4CH_3$); 1.92-2.13(m, 2H, CH_2-dppp).
4	$[Pd(Dmby)_2(dppb)]$	30.03	8.33(s, 2H, CH=N); 7.17-8.14(m, 34H); 6.67-6.92(m, 4H); 2.94-3.18(m, 18H, $2CH_2$-dppb+$4CH_3$); 2.36-2.44(m, 4H, CH_2-2dppb).
5	$[Pd(Dmby)_2(dppf)]$	25.60	8.34(s, 2H, CH=N); 6.52-8.21(m, 38H), 4.41, 4.32(s, 8H, 2Cp-dppf); 3.00(s, 12H, $4CH_3$).
6	$[Pd\ (Dmby)_2(PPh_3)_2]$	25.53	8.38(s, 2H, CH=N); 6.60-8.38(m, 48H); 2.89(s, 12H, $4CH_3$).

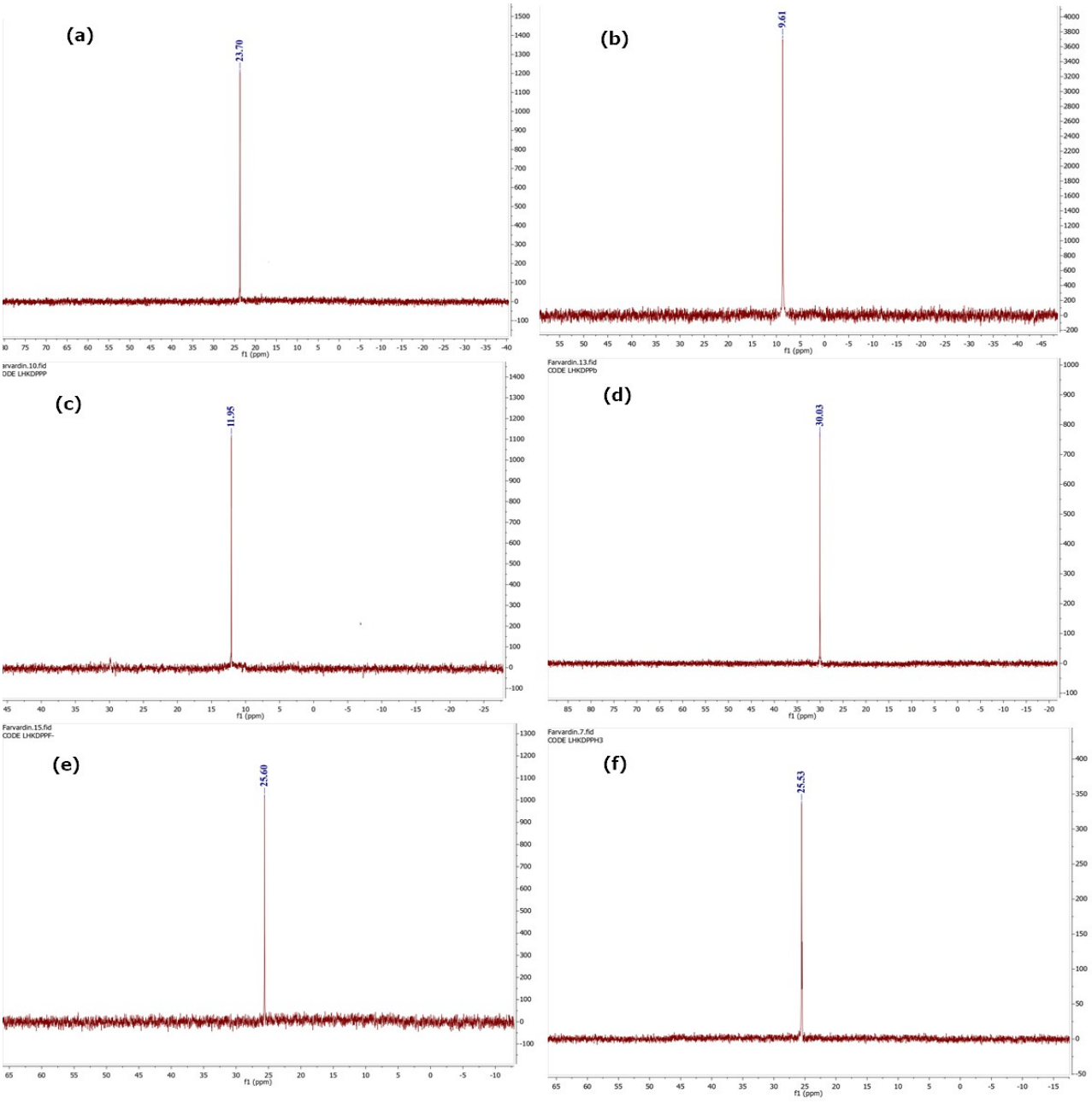

Figure 1: ^{31}P-{^{1}H}NMR spectra of the (a)[Pd(dbeoz)$_2$(dppm)]$_2$, (b) [Pd(dbeoz)$_2$(dppe)], (c) [Pd(dbeoz)$_2$(dppp)], (d)[Pd(dbeoz)$_2$(dppb)], (e)[Pd(dbeoz)$_2$(dppf)] and (f) [Pd(dbeoz)$_2$(PPh$_3$)$_2$].

3.3 Anti-Bacterial Activity Study

The biological activity of the synthesized complexes was evaluated against three pathogenic bacteria *Pseudomonas aeruginosa*, *Bacillus subtilis*, and *Escherichia coli,* using the well diffusion method in the nutrient agar described by Bauer (26).

Six synthesized complexes were evaluated at a concentration of 10^{-3} M in DMSO solution, and the results were compared with Tetracycline and dimethyl sulfoxide (DMSO), which were used as positive and negative controls, respectively. The obtained results were compiled in Table 2, and Figure 4 demonstrates the used compounds as follows:

1. [Pd(dbeoz)$_2$]
2. [Pd(dbeoz)$_2$(dppe)]
3. [Pd(dbeoz)$_2$(dppp)]
4. [Pd(dbeoz)$_2$(dppb)]
5. [Pd(dbeoz)$_2$(dppf)]
6. [Pd (dbeoz)$_2$(PPh$_3$)$_2$]

The results demonstrated that the compounds exhibited inhibitory activity against the studied bacterial strains, as summarized below:

1. The synthesized complexes displayed moderate to good inhibitory activity against the examined bacterial strains compared to the Tetracycline.
2. The complex $[Pd(dbeoz)_2(dppf)]$ exhibited the highest inhibitory activity among the studied complexes, followed by $[Pd(dbeoz)_2(PPh_3)_2]$. This can be attributed to the presence of ferrocenyl and triphenylphosphine ligands.
3. The addition of phosphine ligands to dbeoz complex enhanced inhibitory activity against the tested bacteria.
4. In general, the highest inhibitory activity was observed against *Bacillus subtilis* compared to other bacteria, while the lowest activity was noted against *Pseudomonas aeruginosa*.
5. The inhibitory sequence of the studied complexes in terms of their inhibitory radius was as follows:

$[Pd(Dbeoz)_2(dppf)] > [Pd(Dbeoz)_2(PPh_3)_2] > [Pd(Dbeoz)_2(dppe)] > [Pd(Dbeoz)_2(dppb)] > [Pd(Dbeoz)_2(dppp)] > [Pd(Dbeoz)_2]$ Decreasing inhibition diameter →

Table 4: Diameter inhibition zone (in mm) of the synthesized complexes at 10^{-3} M in DMSO solution.

Seq.	Complexes	DIZ (mm)		
		P. aeruginosa	*B. subtills*	*E. Coli*
1	$[Pd(Dmby)_2]$	13	12	14
2	$[Pd(Dmby)_2(dppe)]$	17	18	18
3	$[Pd(Dmby)_2(dppp)]$	15	14	17
4	$[Pd(Dmby)_2(dppb)]$	15	16	17
5	$[Pd(Dmby)_2(dppf)]$	24	27	28
6	$[Pd\ (Dmby)_2(PPh_3)_2]$	20	21	20
7	Tetracycline	29	30	28

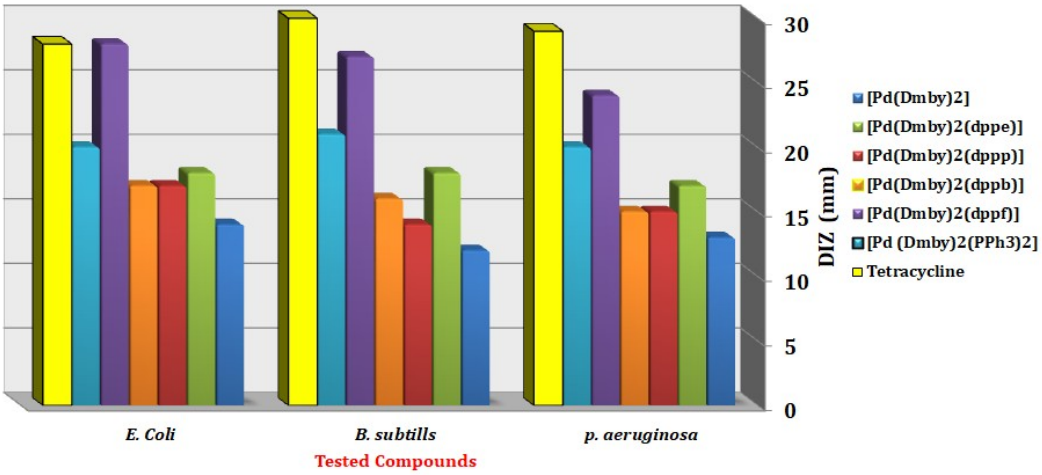

Figure 2. Histogram of the inhibition activity of the synthesized complexes at 10^{-3} M in DMSO solution.

4. CONCLUSION

We demonstrated in this work that $[Pd(dbeoz)_2]$ reacts with phosphine ligands to afford $[Pd(dbeoz)_2(diphos)]$, $[Pd(dbeoz)_2(dppm)]_2$ and $[Pd(dbeoz)_2(PPh_3)_2]$ **(1-6)** in which dbeoz acts as a monodentate through the oxygen atom of the carbonyl group. The prepared complexes were characterized by different spectroscopic and physical methods. Further, the biological activity of the synthesized complexes was screened against *Pseudomonas aeruginosa*, *Bacillus subtilis*, and *Escherichia coli* bacteria species, and the complexes showed moderate to good inhibitory activity, and the $[Pd(dbeoz)_2(dppf)]$ complex has a highest inhibitory activity.

5. REFERENCES

1. Shakdofa MME, Shtaiwi MH, Morsy N, Abdel-rassel TMA. Metal complexes of hydrazones and their biological, analytical and catalytic applications: A review. Main Group Chemistry. 2014;13(3):187–218. Available from: <URL>.

2. Kumar M, Roy S, Faizi MdSH, Kumar S, Singh MK, Kishor S, et al. Synthesis, crystal structure and luminescence properties of acenaphthene benzohydrazide based ligand and its zinc(II) complex. Journal of Molecular Structure. 2017 Jan;1128:195–204. Available from: <URL>.

3. Tabernero V, Cuenca T, Herdtweck E. Hydrazonide titanium derivatives. Journal of Organometallic Chemistry. 2002 Dec;663(1–2):173–82. Available from: <URL>.

4. Pelagatti P, Carcelli M, Pelizzi C, Costa M. Polymerisation of phenylacetylene in water catalysed by Pd(NN'O)Cl complexes. Inorganica Chimica Acta. 2003 Jan;342:323–6. Available from: <URL>.

5. Chen L. Ethylene oligomerization by hydrazone Ni(II) complexes/MAO. Applied Catalysis A: General. 2003 Jun 25;246(1):11–6. Available from: <URL>.

6. Zhong X, Wei HL, Liu WS, Wang DQ, Wang X. The crystal structures of copper(II), manganese(II), and nickel(II) complexes of a (Z)-2-hydroxy-N'-(2-oxoindolin-3-ylidene) benzohydrazide—potential antitumor agents. Bioorganic & Medicinal Chemistry Letters. 2007 Jul;17(13):3774–7. Available from: <URL>.

7. Cullen STJ, Friestad GK. Alkyl Radical Addition to Aliphatic and Aromatic N -Acylhydrazones Using an Organic Photoredox Catalyst. Organic Letters. 2019 Oct 18;21(20):8290–4. Available from: <URL>.

8. Kvasovs N, Gevorgyan V. Accessing Illusive E Isomers of α-Ester Hydrazones via Visible-Light-Induced Pd-Catalyzed Heck-Type Alkylation. Organic Letters. 2022 Jun 17;24(23):4176–81. Available from: <URL>.

9. Prieto A, Bouyssi D, Monteiro N. Radical-Mediated Formal C(sp 2)–H Functionalization of Aldehyde-Derived N , N -Dialkylhydrazones. European Journal of Organic Chemistry. 2018 Jun 7;2018(20–21):2378–93. Available from: <URL>.

10. Xu X, Zhang J, Xia H, Wu J. C(sp 2)–H functionalization of aldehyde-derived hydrazones via a radical process. Organic and Biomolecular Chemistry. 2018;16(8):1227–41. Available from: <URL>.

11. El-Tabl AS, Mohamed Abd El-Waheed M, Wahba MA, Abd El-Halim Abou El-Fadl N. Synthesis, Characterization, and Anticancer Activity of New Metal Complexes Derived from 2-Hydroxy-3-(hydroxyimino)-4-oxopentan-2-ylidene)benzohydrazide. Bioinorganic Chemistry and Applications. 2015;2015:1–14. Available from: <URL>.

12. Okagu OD, Ugwu KC, Ibeji CU, Ekennia AC, Okpareke OC, Ezeorah CJ, et al. Synthesis and characterization of Cu(II), Co(II) and Ni(II) complexes of a benzohydrazone derivative: Spectroscopic, DFT, antipathogenic and DNA binding studies. Journal of Molecular Structure. 2019 May;1183:107–17. Available from: <URL>.

13. Katouah HA, Al-Fahemi JH, Elghalban MG, Saad FA, Althagafi IA, El-Metwaly NM, et al. Synthesis of new Cu(II)-benzohydrazide nanometer complexes, spectral, modeling, CT-DNA binding with potential anti-inflammatory and anti-allergic theoretical features. Materials Science and Engineering: C. 2019 Mar;96:740–56. Available from: <URL>.

14. Al-Qadsy I, Al-Odayni AB, Saeed WS, Alrabie A, Al-Adhreai A, Al-Faqeeh LAS, et al. Synthesis, Characterization, Single-Crystal X-ray Structure and Biological Activities of [(Z)-N'-(4-Methoxybenzylidene) benzohydrazide–Nickel(II)] Complex. Crystals. 2021 Jan 26;11(2):110. Available from: <URL>.

15. Korkmaz IN, Türkeş C, Demir Y, Öztekin A, Özdemir H, Beydemir Ş. Biological evaluation and in silico study of benzohydrazide derivatives as paraoxonase 1 inhibitors. J Biochemistry & Molecular Toxicity. 2022 Nov;36(11):e23180. Available from: <URL>.

16. Zuo W, Tourbillon C, Rosa V, Cheaib K, Andrade MM, Dagorne S, et al. Synthesis, crystal structures and use in ethylene oligomerization catalysis of novel mono- and dinuclear nickel complexes supported by (E)-N'-(1-(thiophen-2-yl)ethylidene)benzohydrazide ligand. Inorganica Chimica Acta. 2012 Mar;383:213–9. Available from: <URL>.

17. Burgos-Lopez Y, Del Plá J, Balsa LM, León IE, Echeverría GA, Piro OE, et al. Synthesis, crystal structure and cytotoxicity assays of a copper(II) nitrate complex with a tridentate ONO acylhydrazone ligand. Spectroscopic and theoretical studies of the complex and its ligand. Inorganica Chimica Acta. 2019 Mar;487:31–40. Available from: <URL>.

18. Theppitak C, Kielar F, Dungkaew W, Sukwattanasinitt M, Kangkaew L, Sahasithiwat S, et al. The coordination chemistry of benzhydrazide with lanthanide(iii) ions: hydrothermal in situ ligand formation, structures, magnetic and photoluminescence sensing properties. RSC Advances. 2021;11(40):24709–21. Available from: <URL>.

19. Guan Q, Zhou LL, Dong YB. Metalated covalent organic frameworks: from synthetic strategies to diverse applications. Chemical Society Reviews. 2022; 51(15):6307–416. Available from: <URL>.

20. Zhao J, Yuan J, Fang Z, Huang S, Chen Z, Qiu F, et al. One-dimensional coordination polymers based on metal–nitrogen linkages. Coordination Chemistry Reviews. 2022 Nov;471:214735. Available from: <URL>.

21. Sánchez-Fernández JA. Structural Strategies of Supramolecular Hydrogels and Their Applications [Internet]. Chemistry; 2023 Feb [cited 2023 Dec 1]. Available from: <URL>.

22. Bauer AW. Single-Disk Antibiotic-Sensitivity Testing of Staphylococci: An Analysis of Technique and Results. JAMA Internal Medicine. 1959 Aug 1;104(2):208. Available from: <URL>.

23. Mohamed DS, Al-Jibori SA, Behjatmanesh-Ardakani R, Faihan AS, Yousef TA, Alhamzani AG, et al. Spectroscopic, Anti-Cancer Activity, and DFT Computational Studies of Pt(II) Complexes with 1-Benzyl-3-phenylthiourea and Phosphine/Diamine Ligands. Inorganics. 2023 Mar 16;11(3):125. Available from: <URL>.

24. Al-Janabi ASM, Yousef TA, Al-Doori MEA, Bedier RA, Ahmed BM. Palladium(II)-salicylanilide complexes as antibacterial agents: Synthesis, spectroscopic, structural characterization, DFT calculations, biological and in silico studies. Journal of Molecular Structure. 2021 Dec;1246:131035. Available from:<URL>.

25. Al-Jibori SA, Al-Jibori GHH, Saleh SS, Al-Janabi AS, Laguna M, Wagner C. Mercury (II) benzisothiazolinate (bit) complexes with diamine or phosphine co-ligands, and subsequent conversion to 2-mercaptobenzamide complexes. Crystal structures of [Hg(bit)2(L2)], L2 = bipyridine or phenanthroline. Polyhedron. 2021 Sep;206:115353. Available from: <URL>.

26. Salih MM, Saleh AM, Hamad AS, Al-Janabi AS. Synthesis, spectroscopic, anti-bacterial activity, molecular docking, ADMET, toxicity and DNA binding studies of divalent metal complexes of pyrazole-3-one azo ligand. Journal of Molecular Structure. 2022 Sep;1264:133252. Available from: <URL>.

27. Al-Janabi ASM, Oudah KH, Aldossari SA, Khalaf MA, M. Saleh A, Hatshan MR, et al. Spectroscopic, anti-bacterial, anti-cancer and molecular docking of Pd(II) and Pt(II) complexes with (E)-4-((dimethylamino)methyl)-2-((4,5-dimethylthiazol-2-yl)diazenyl)phenol ligand. Journal of Saudi Chemical Society. 2023 May;27(3):101619. Available from: <URL>.

28. Afandi ZS, Al-Jibori SA, Ferjani H, Al-Shammar RH, Aldossari SA, Al-Janabi AS. Ortho-palladated complexes with aromatic N-donor ligands, synthesis, characterization, molecular structures, antibacterial and anticancer activity [Internet]. In Review; 2022 Oct [cited 2023 Dec 1]. Available from: <URL>.

29. Al-Janabi ASM, Elzupir AO, Abou-Krisha MM, Yousef TA. New Dual Inhibitors of SARS-CoV-2 Based on Metal Complexes with Schiff-Base 4-Chloro-3-Methyl Phenyl Hydrazine: Synthesis, DFT, Antibacterial Properties and Molecular Docking Studies. Inorganics. 2023 Jan 29;11(2):63. Available from: <URL>.

30. Al-Janabi AMA, Faihan AS, Al-Mutairi AM, Hatshan MR, Al-Jibori SA, Al-Janabi ASM. Spectroscopic, biological activity studies, and DFT calculations, of Pd(II) and Pt(II) complexes of 4-Methylene-3-phenyl-3,4-dihydroquinazoline-2(1H)-thione. Journal of the Indian Chemical Society. 2022 Nov;99(11):100774. Available from: <URL>.

31. Al-Jibori LH, Al-Janabi AS. Spectroscopic characterization, and anti-bacterial activity studies of the benzohydrazide derivatives complexes. Microbial Science Archives. 2023;3(3):141–6.